

Numerical Analysis of Unsteady Conjugate Heat Transfer for Initial Evolution of Thermal Stratification in a Curved Pipe

Jong Chull Jo, Wee Kyung Kim, Yun Il Kim and Sang Jin Cho

Korea Institute of Nuclear Safety
19 Kusung-dong, Yusung-ku, Taejon 305-338, Korea

Seok Ki Choi

Korea Atomic Energy Research Institute
150 Dukjin-dong, Yusung-ku, Taejon 305-353, Korea

Abstract

A detailed numerical analysis of initial evolution of thermal stratification in a curved pipe with a finite wall thickness is performed. A primary emphasis of the present study is placed on the investigation of the effect of existence of pipe wall thickness on the evolution of thermal stratification. A simple and convenient numerical method of treating the unsteady conjugate heat transfer in Cartesian as well as non-orthogonal coordinate systems is presented. The proposed unsteady conjugate heat transfer analysis method is implemented in a finite volume thermal-hydraulic computer code based on a cell-centered, non-staggered grid arrangement, the SIMPLER algorithm and a higher-order bounded convection scheme. Calculations are performed for initial evolution of thermal stratification with high Richardson number in a curved pipe. The predicted results show that the thermally stratified flow and transient conjugate heat transfer in a curved pipe with a specified wall thickness can be satisfactorily analyzed by using the numerical method presented in this paper. As the result, the present analysis method is considered to be effective for the determination of transient temperature distributions in the wall of curved piping system subjected to internally thermal stratification. In addition, the method can be extended to be applicable for the simulation of turbulent flow of thermally stratified fluid.

1. Introduction

Some safety-related piping systems connected to reactor coolant systems at operating nuclear power plants are known to be potentially susceptible to unanticipated flow-induced thermal stratification which can lead to thermal fatigue damage to the piping systems. Several plants have so far experienced such serious mechanical damages due to thermal fatigue such as pressurizer surge line movements and its support failures, and cracks in feedwater nozzle, high pressure safety injection lines, and residual heat removal lines. Thus, the understanding of thermal stratification phenomenon in the components of nuclear power plant is very important for securing the structural integrity and safety of nuclear power plant.

The temperature difference in the fluid region due to the thermal stratification produces thermal stress in the pipe both in axial and circumferential directions. Several investigators have made efforts to determine the temperature distributions in the pipe wall by means of laboratory testing of particular geometry, field measurement of temperature or fully theoretical predictions [1-5]. Abou and Barois [6] and Baron et al. [7] have made numerical calculations for stratified pipe flow in pressurized water reactor (PWR) using the $k-e$ turbulence model and curvilinear coordinates. Reasonably good agreements are observed between measurement and calculated results. Baik et al. [8] have carried out unsteady, three-dimensional calculations for analyzing thermal stratification in the surge line of the Korean next generation reactor using the commercial code. A parametric study has been carried out to investigate the effect of inlet velocity, temperature difference and pipe slope on the development of thermal stratification.

However, most of previous authors neglected the existence of pipe wall thickness. Most of pipes in the nuclear power plant have a thick pipe wall to take into account of the wall thinning effect during the long time operation. For example, the wall thickness in the pipe of the pressurizer surge line of PWR in which the

thermal stratification occurs is about 0.3 times the inner radius of pipe. In order to understand the effect of thermal stratification on the pipe wall and to evaluate the thermal stress caused by the thermal stratification, the temperature distribution inside the thick pipe wall must be calculated. The primary objective of present study is to investigate the evolution of temperature field inside the thick pipe wall during the formation of thermal stratification.

When the conducting solid material is included in the solution domain of fluid flow and heat transfer, the problem is usually called the conjugate heat transfer problem. Although several conjugate heat transfer calculations are performed so far, it is very difficult to find a clear documentation of methodology of analysis of unsteady conjugate heat transfer in a non-orthogonal coordinate system. A very simple and convenient way of treating the conjugate heat transfer in a Cartesian and non-orthogonal coordinates is presented in the present study employing the equivalent conductivity concept developed by Patankar [9].

The piping systems in a nuclear power plant have complicated shaped boundaries, which requires the use of non-orthogonal curvilinear coordinates for the numerical solution of fluid flow and heat transfer inside the piping system. For this purpose, a three-dimensional thermal-hydraulic computer code for analyzing the thermally stratified flows in a curved piping system has been developed using a body-fitted, non-orthogonal curvilinear coordinate. The cell-centered, non-staggered grid arrangement is adopted and the resulting checkerboard pressure oscillation is prevented by the application of momentum interpolation method [10]. The SIMPLEX algorithm [11] is employed for the pressure and velocity coupling. The convection term is approximated by a higher-order bounded convection scheme.

To the present author's knowledge there does not exist a detailed measurement that shows the evolution of thermal stratification in the piping systems and can be used for validation of thermal-hydraulic computer codes. Ushijima [12] has provided some experimental measurements which show the transient evolution of temperature field in a curved duct. Ushijima [12] did not take into account the wall thickness effect. The computer code developed on the basis of the present numerical analysis method has been well validated in literatures [13, 14] by comparing the calculation results for the non-conjugate problem of curved duct, of which the effect of wall thickness is not considered, with the measured data of Ushijima [12].

The main objective of present study is to investigate the effect of existence of pipe wall thickness on the transient evolution of thermal stratification in a curved pipe. For this purpose a simple and convenient numerical method of treating unsteady conjugate heat transfer in a non-orthogonal coordinate is proposed, and is implemented in a thermal-hydraulic computer code developed for analysis of fluid flow and heat transfer in a complex geometry. Calculations are performed for the transient evolution of thermal stratification in a curve pipe with finite wall thickness. The predicted results for the evolution of temperature fields of fluid and pipe wall are presented to understand how the existence of a finite thick wall affects the evolution of temperature field.

2. Mathematical Formulation and Numerical Method

Governing equations

For simplicity, it is assumed the thermally stratified fluids is Newtonian with constant properties and the Boussinesq approximation is valid. Then the governing equations for conservation of mass, momentum and energy in a generalized coordinate system x^j can be written as follows [15],

$$\frac{\partial}{\partial x^j}(U_j) = 0 \quad (1)$$

$$\frac{\partial}{\partial t}(J\mathbf{r}u_i) + \frac{\partial}{\partial x^j} \left[U_j u_i - \frac{\mathbf{m}}{J} \left\{ \frac{\partial u_i}{\partial x^m} B_m^j + b_k^j w_i^k \right\} + P b_i^j \right] = \mathbf{r}g_i \mathbf{b}(T - T_{ref})J \quad (2)$$

$$\frac{\partial}{\partial t}(J\mathbf{r}C_p T) + \frac{\partial}{\partial x^j} \left[U_j C_p T - \frac{k}{J} \frac{\partial T}{\partial x^m} B_m^j \right] = 0 \quad (3)$$

$$\text{where} \quad U_i = \mathbf{r}u_k b_k^i, \quad B_m^j = b_k^j b_k^m, \quad w_j^i = \frac{\partial u_i}{\partial x^k} b_j^k \quad (4)$$

and u_i denotes the three Cartesian velocity components in the directions of the transformed coordinates $y^i = y^i(x^j)$, the geometric coefficients b_i^j represent the cofactors of $\partial y^i / \partial x^j$ in the Jacobian matrix of the coordinate transformation, J stands for the determinant of the Jacobian matrix and y^i is the Cartesian coordinate system.

Initial and boundary conditions

Consider a general situation of thermally stratified flow in a curved pipe with a finite wall thickness. A fluid of the high temperature is flowing through the pipe at a constant flow rate so that the steady flow condition is maintained, and then the inlet temperature is lowered at a certain point of time. Because the solution domain is symmetric geometrically, only half of the solution domain is solved. Thus, at the symmetry plane, the symmetry boundary conditions are applied for both velocity components and temperature. At the outer wall the adiabatic condition is specified. For this situation the boundary conditions are given by

$$u_i = u_{i,in}, \quad T = T_{in} \quad \text{at the inlet of the pipe,} \quad (5)$$

$$\left. \frac{\partial T}{\partial n} \right|_{x^2} = 0 \quad \text{at the outer wall of the pipe} \quad (6)$$

$$u_2 = 0, \quad \frac{\partial u_1}{\partial x^3} = \frac{\partial u_3}{\partial x^3} = 0, \quad \frac{\partial T}{\partial x^3} = 0 \quad \text{at the symmetry plane} \quad (7)$$

$$\left. \frac{\partial T}{\partial x^1} \right| = 0 \quad \text{at the outlet of the pipe} \quad (8)$$

At the outlet, the velocity components are adjusted to satisfy the overall mass conservation.

Numerical methods

The solution domain is divided into a finite number of hexahedral control volume cells. The discretization of the governing equations is performed following the finite volume approach. The convection terms are approximated by a higher-order bounded scheme HPLA developed by Zhu [16] and the unsteady term is treated implicitly using the three-level second order scheme suggested by Ferziger and Peric [17]. The cell-centered, non-staggered grid arrangement is adopted in the present study. The momentum equations and energy equation are solved implicitly at the cell-centered locations. The resulting checkerboard pressure oscillation is prevented by the application of momentum interpolation method proposed by Rhie and Chow [10]. The original Rhie and Chow scheme is further modified to obtain a converged solution for unsteady flows which is independent of the size of time step and relaxation factors as was modified by Majumdar [18] and Choi [19].

3. Numerical Treatment of Unsteady Conjugate Heat Transfer

For the sake of simplicity consider an unsteady two-dimensional conjugate heat transfer problem. The energy equation in a Cartesian coordinate system with temperature as dependent variable can be written as follows,

$$\frac{\partial}{\partial t}(\mathbf{r}_f C_{P_f} T) + \frac{\partial}{\partial x_j}(\mathbf{r}_f C_{P_f} u_j T) = \frac{\partial}{\partial x_j} \left(k_f \frac{\partial T}{\partial x_j} \right) \quad \text{in fluid regions} \quad (9)$$

$$\frac{\partial}{\partial t}(\mathbf{r}_s C_{P_s} T) = \frac{\partial}{\partial x_j} \left(k_s \frac{\partial T}{\partial x_j} \right) \quad \text{in solid regions} \quad (10)$$

At the fluid-solid interface the following continuous heat flux condition is satisfied.

$$-k_f \left. \frac{\partial T}{\partial x} \right|_i = -k_s \left. \frac{\partial T}{\partial x} \right|_i \quad (11)$$

Following the notations given in Fig.1, above boundary condition can be rewritten in a discretized form as follows,

$$-k_f \frac{T_i - T_f}{\mathbf{D}x_f} = -k_s \frac{T_s - T_i}{\mathbf{D}x_s} \quad (12)$$

Manipulation of above equation gives the value of temperature at the fluid-solid interface.

$$T_i = \frac{1}{\mathbf{D}x_s k_f + \mathbf{D}x_f k_s} (\mathbf{D}x_f k_s T_s + \mathbf{D}x_s k_f T_f) \quad (13)$$

A straightforward way of solving the conjugate heat transfer problem is solving Eq.(9) and Eq.(10) separately using the interface temperature T_i as the temperature boundary condition at the fluid-solid interface. However, this practice requires a separate solution of energy equation in solid and fluid regions and the computer program becomes complicated and it is very difficult to implement this practice in a general purpose computer code. To avoid this difficulty, Patankar [9] introduced an equivalent conductivity concept which enables to solve the energy equation in fluid and solid regions simultaneously.

Using the interface temperature given in Eq.(13) the heat flux at the fluid-solid interface can be expressed in terms of T_s and T_f as follows,

$$q_i = -k_{eq} \frac{T_s - T_f}{x_s - x_f} \quad (14)$$

where

$$k_{eq} = \frac{k_s k_f}{(1 - f_i)k_f + f_i k_s} \quad (15)$$

$$f_i = \frac{\mathbf{D}x_f}{\mathbf{D}x_s + \mathbf{D}x_f} \quad (16)$$

We note that the equivalent conductivity, k_{eq} in Eq.(15), is the harmonic mean of k_f and k_s if the numerical grid is uniform. Since the Eq.(14) is derived from Eq.(11), the continuous heat flux condition is satisfied if we use k_{eq} as the diffusion coefficient for the energy equation at the fluid-solid interface. The physical effectiveness of this equivalent conductivity is well explained in Patankar [9].

By introducing the equivalent conductivity concept, the energy equations in fluid and solid regions can be solved simultaneously. However, the existence of C_{P_f} and C_{P_s} in the convection and unsteady terms requires a careful programming in solving the energy equation. If we divide C_{P_f} for Eq.(9) and C_{P_s} for Eq.(10) to avoid this problem and if we introduce the equivalent diffusivity at the interface as the same way described before, the continuous heat flux condition at the interface will not be satisfied unless C_{P_s} is equal to C_{P_f} . To avoid this problem we divided C_{P_f} for both Eq.(9) and Eq.(10). Then, the continuous heat flux condition at the fluid-solid interface will be satisfied. After some manipulations, the resulting energy equation can be written as follows,

$$\frac{\partial}{\partial t}(\mathbf{r}_f T) + \frac{\partial}{\partial x_j}(\mathbf{r}_f u_j T) = \frac{\partial}{\partial x_j} \left(\frac{\mathbf{m}_f}{\text{Pr}_f} \frac{\partial T}{\partial x_j} \right) \quad \text{in fluid regions} \quad (17)$$

$$\frac{\partial}{\partial t}(\mathbf{r}_f \mathbf{r}_{fact} T) = \frac{\partial}{\partial x_j} \left(\frac{\mathbf{m}_f}{\text{Pr}_f} \mathbf{G}_{fact} \frac{\partial T}{\partial x_j} \right) \quad \text{in solid regions} \quad (18)$$

where

$$\mathbf{r}_{fact} = \begin{pmatrix} \mathbf{a}_f \\ \mathbf{a}_s \end{pmatrix} \begin{pmatrix} k_s \\ k_f \end{pmatrix} \quad (19)$$

$$\mathbf{G}_{fact} = \begin{pmatrix} k_s \\ k_f \end{pmatrix} \quad (20)$$

We note that the Eq.(17) is the same as the general form of energy equation commonly used in the computational fluid dynamics, especially in the SIMPLE family of solution methods. From above equations we can notice that the only things we have to do in the solution of conjugate heat transfer is the multiplication of \mathbf{r}_{fact} and \mathbf{G}_{fact} to the density and diffusion coefficient of fluid respectively in the solid region and the introduction of equivalent diffusion coefficient at the fluid-solid interface as is done in Eq.(15). To the present author's knowledge this simple and convenient way of treating the unsteady conjugate heat transfer is not reported in the literatures

When the numerical grid is non-orthogonal, the continuous heat flux condition at the fluid-solid interface can be written as follows,

$$-k_f \nabla T \cdot \mathbf{n} = -k_s \nabla T \cdot \mathbf{n} \quad (21)$$

Following the notations given in Fig.2, the equivalent conductivity at the fluid-solid interface in a non-orthogonal grid situation can be derived exactly the same way as is done in the Cartesian coordinate system.

$$k_{eq} = \frac{C_1 C_2 (T_s - T_f) + C_1 C_4 + C_2 C_3}{(C_1 + C_2)[(T_s - T_f)C_5 + C_6]} \quad (22)$$

where

$$\begin{aligned} C_1 &= k_f \frac{(e^1 \cdot n)_f}{(\mathbf{D}\mathbf{x})_f}, & C_2 &= k_s \frac{(e^1 \cdot n)_s}{(\mathbf{D}\mathbf{x})_s}, & C_3 &= k_f \frac{(T_{i2} - T_{i1})}{(\mathbf{D}\mathbf{h})_f} (e^2 \cdot n)_f, \\ C_4 &= k_s \frac{(T_{i2} - T_{i1})}{(\mathbf{D}\mathbf{h})_s} (e^2 \cdot n)_s, & C_5 &= \frac{(e^1 \cdot n)}{\mathbf{D}\mathbf{x}}, & C_6 &= \frac{(T_{i2} - T_{i1})}{\mathbf{D}\mathbf{h}} (e^2 \cdot n) \end{aligned} \quad (23)$$

$$e^1 = \frac{1}{J} \left(\frac{\partial y}{\partial \mathbf{h}} i - \frac{\partial x}{\partial \mathbf{h}} j \right), \quad e^2 = \frac{1}{J} \left(-\frac{\partial y}{\partial \mathbf{x}} i + \frac{\partial x}{\partial \mathbf{x}} j \right) \quad (24)$$

$$J = \frac{\partial x}{\partial \mathbf{x}} \frac{\partial y}{\partial \mathbf{h}} - \frac{\partial x}{\partial \mathbf{h}} \frac{\partial y}{\partial \mathbf{x}} \quad (25)$$

$$\mathbf{D}\mathbf{x} = (\mathbf{D}\mathbf{x})_f + (\mathbf{D}\mathbf{x})_s \quad (26)$$

We note that the equivalent conductivity in a non-orthogonal grid situation is coupled with the temperature due to the non-orthogonality of numerical grid. However, it does not make any problems since the energy equation is solved iteratively at each time step. The equivalent conductivity is updated at each iteration level using the newly updated temperature field. The extension of above formulation in a three-dimensional non-orthogonal grid situation is straightforward and is not presented here due to the complexity of the formulation.

4. Results and Discussion

The numerical solution method presented in the present study is applied to the analysis of thermal stratification in a curved pipe and calculations are performed for symmetric half of the solution domain. The $74 \times 27 \times 36$ numerical grids are generated algebraically as shown in Fig.1. The Reynolds number based on the hydraulic diameter of the pipe and the inlet velocity is 1040, and the Richardson number is around 12000.

Since the Richardson number is very high, the buoyancy force affects strongly the flow field. First, the steady state solution is obtained with the temperature maintained at high temperature and then the transient solutions are obtained using the steady state solution as an initial condition. The inlet temperature is assumed to lower instantly by 10 degrees at the moment when the transient begins. Calculations are continued until 600 seconds using the time step size of 0.1 second. The convergence is declared at each time step when the maximum of the absolute sum of the residuals of momentum equations, pressure correction equation and energy equation is less than 10^{-4} .

Before investigating a detailed evolution of thermal stratification in a curved pipe, a primary calculation was performed to validate the computer code for the duct flow (Reynolds number of 500 and Richardson number of 9.8) studied experimentally by Ushijima [12], where the inlet temperature is assumed to be lowered linearly by 10 degrees during the initial 30 seconds and the wall thickness of duct is considered to be so small that the effect is negligible. Fig. 2 displays the comparison of predicted temperature distribution at the symmetry plane and with the measured data by Ushijima [12]. Fig. 3 shows the comparison of calculated results with measured data for vertical temperature distribution at $t=120$ sec for three sections at the symmetry plane (section A: end of first curved section, section B: center plane, section C: start of second curved section). We observe from the figures 2 and 3 that the numerically predicted results fairly well agree with the experimental measurements, especially when the thermal stratification is established ($t=120$ sec), except that the numerically predicted thermal interface is located slightly higher than that of experimental measurement. Those small discrepancies may be due to the differences in inlet conditions between measurement and calculation, which can be observed in the initial development of temperature in the measured data. However, we can notice that a slightly different imposition of inlet temperature in the initial period of time does not much influence the final formation of thermal stratification. As confirmed in the previous study [13] that the predictions by the present approach agree fairly well with the predictions by Ushijima [12]. Some discrepancies may be due to the use of different numerical method and numerical grids.

Fig. 4 shows the transient evolution of temperature field at the symmetry plane for the pipe flow under

consideration. The predicted temperature field is normalized using the hot temperature and cold temperature, and the interval of the isothermal line is 0.1. In the initial stage ($t \approx 20$ sec) the inlet flow moves upward pushing the hot fluid in the downstream direction. When the cold fluid reaches the first curved section, it begins to flow into the lower side of the pipe with the force balance between inertia of inlet flow and buoyancy of hot water. Even the cold fluid moves further downstream and reaches the outlet ($t=30$ sec), the temperature of fluid in the upper portion of the pipe does not change and a steep temperature gradient is established at the interface between hot and cold fluid regions. The temperature gradient at the interface becomes steeper as time elapses and there exists a strong mixing near the outlet ($t=30\sim 50$ sec). A stable thermal stratification begins to be established in the upper portion of the pipe ($t=100\sim 400$ sec), and then the mixing near the outlet is finished and the stable thermal stratification does not change much with time ($t=600$ sec). Since the Richardson number of the present problem is very high, the thermally stratified region covers for most upper portion of the pipe. One thing we note here is that the cold fluid does not mix well with the hot fluid once the thermal stratification is established.

Fig. 5 displays the predicted isothermal lines at the cross section of the center plane of the pipe. These figures show well the development of the thermal stratification. At an earlier stage of the mixing process the temperature gradient near the lower wall is small and a little strange evolution of the temperature field in this region is due to the soaking of cold fluid, which can be seen in Fig. 6. The temperature gradient at the interface between cold fluid and hot fluid becomes steeper as the stratification is established ($t=30$ sec). A steep temperature gradient is established around $t=50$ sec. Then the temperature gradient at the upper portion of the interface becomes smaller ($t=400\sim 600$ sec) due to the heat transfer at the interface of hot and cold fluids.

To assess the potential for piping damage due to the thermal stratification, it is necessary, first of all, to determine the transient temperature distributions in the wall of the pipe in which thermally stratified flow exists. As can be seen in Figs. 4-5, the present calculations provide the transient temperature distributions in the wall of the reversed U-pipe. Initially, the pipe wall is maintained at the same temperature as that of the hot fluid flowing through the pipe. As the cold fluid begins to flow through the pipe resulting in thermal stratification, the part of pipe wall contacting with the cold fluid decreases so that the temperature gradients at and around the locations of pipe inner wall wetted by the fluid interface between the stratified fluid become steep. Those steep temperature gradients are formed concurrently in the longitudinal, circumferential and radial directions for the duration of thermal stratification. It is also shown in Figs. 4-5 that the temperature gradient in the radial direction is very steep at the early stage of thermal stratification is very steep and becomes easy as the time elapses. On the contrary, the temperature gradient in the circumferential direction is not severe at the early stage of stratification but it become steep gradually as the thermal stratification evolves and finally reaches its maximum after a stable thermal stratification begins to be established in the upper portion of the pipe.

Fig. 6 shows the development of velocity vectors at the symmetry plane. At the initial stage, the velocity field is not changed much compared with the initial steady state solution. When the thermal stratification is begun to form balancing the inertia and buoyancy forces, the magnitude of fluid flows near the lower side of pipe becomes larger ($t=30$ sec). There is a strong movement of cold fluid when the cold fluid passes the second curved section ($t=50$ sec) since the incoming cold fluid could not penetrate into the hot fluid region. The strong movement of cold fluid pushes the existing hot fluid in both upward and downward directions and it induces a counterclockwise movement of hot fluid in upper region of the pipe and a strong clockwise vortex near the outlet ($t=30\sim 50$ sec). There exists a strong mixing near the outlet of the pipe. As the time elapses, the cold fluid flows into the outlet mixing with hot fluid and the counterclockwise vortex in the upper right region of the pipe becomes weak ($t=100$ sec). There still exists a mixing near the outlet and the flow in this region is developing while the flow in upper region of the pipe is nearly quiescent ($t=100\sim 400$ sec). When the mixing process near the outlet is finished, the velocity field in this region as well as other region is nearly developed ($t=600$ sec). We can see that the development of velocity field is consistent with that of temperature field.

Fig. 7 displays the development of a secondary motion at the cross-section of the center plane of the pipe. There exists a relatively strong vortex initially ($t=30$ sec) and the magnitude of vortex becomes weak as the mixing process continues ($t=30\sim 50$ sec). Then the secondary motion changes rapidly ($t=30\sim 50$ sec) and the complicated evolution of secondary motion are continued until a stable stratification is established ($t=100$ sec). After the stable stratification is established, the secondary motion in the hot fluid region is very weak and there exists a strong clockwise vortex at the bottom of the pipe due to the relatively high strength of the primary motion in this region.

From the above investigations, it is seen that the present numerical analysis method is effective to solve the unsteady flow and conjugate heat transfer in a curved pipe subjected to internally thermal stratification. In addition, the computer code is considered to be valid for calculating the transient temperature distributions in the piping wall, which are needed as input data in the thermal stress analysis of the pipe.

5. Conclusions

A detailed numerical analysis of initial evolution of thermal stratification in a curved pipe with a finite wall thickness has been performed. A main emphasis of the present study has been placed on the investigation of the effect of existence of pipe wall thickness on the evolution of thermal stratification. A simple and convenient numerical method of treating the unsteady conjugate heat transfer in Cartesian as well as non-orthogonal coordinate systems has been presented. The proposed unsteady conjugate heat transfer analysis method has been implemented in a finite volume thermal-hydraulic computer code based on a cell-centered, non-staggered grid arrangement, the SIMPLEC algorithm and a higher-order bounded convection scheme. Calculations have been performed for initial evolution of thermal stratification with high Richardson number in a curved pipe. The predicted results showed that the thermally stratified flow and transient conjugate heat transfer in a curved pipe with a specified wall thickness can be satisfactorily analyzed by using the numerical method presented in this paper. As the result, it is seen that the transient behaviors of thermally stratified flows in curved pipes with specified thickness can be well simulated by the present analysis method and the method is considered to be effective for the determination of transient temperature distributions in the wall of curved piping system subjected to internally thermal stratification. In addition, the present method can be extended to be applicable for the simulation of turbulent flow of thermally stratified fluids.

Consequently, the favorable results show that the present computer code can be applied to the prediction of practical thermal stratification phenomena in a nuclear power plant. The thermal stratification in a practical nuclear power plant involves turbulent flow, temperature gradient, oscillations of the stratification interface and inherent local temperature fluctuations. Time-variations of the temperature due to the turbulent fluctuations can be as critical as the spatial variations. In this case the large eddy simulation method can be an attractive method of predicting instantaneous flow topology, time-dependent turbulent interaction and therefore the temperature fluctuation.

Nomenclature

b_i^j	cofactors of $\partial y^i / \partial x^j$ in the Jacobian matrix of coordinate transformation
B_m^j	geometric coefficient defined in Eq.(4)
C_1, C_2, \dots, C_6	coefficients defined in Eq.(23) to Eq.(25)
C_p	specific heat
e^1, e^2	contravariant base vectors
f_i	geometric interpolation factor defined in Eq.(16)
g_i	acceleration of gravity in i -direction
i, j	Cartesian base vectors
J	determinant of Jacobian matrix of coordinate transformation
k	conductivity
n	normal vector
P	pressure
Pr	Prandtl number
q	heat flux
Ri	Richardson number ($Ri = \frac{g \mathbf{b} (T_h - T_c)}{u_{in}^2}$)
t	time
T	temperature
u_i	Cartesian velocity components
u_{in}	inlet velocity of pipe flow
U_j	mass flux defined in Eq.(4)
w_j^i	terms defined in Eq.(4)
$(x, y), (x_1, x_2)$	Cartesian coordinates in two dimensional case
x^j	generalized coordinate system

y^i	Cartesian coordinate system
\mathbf{a}	thermal diffusivity ($= \frac{k}{\rho C_p}$)
\mathbf{b}	volumetric coefficient of thermal expansion
∇	gradient
\mathbf{m}	viscosity
\mathbf{G}_{fact}	multiplication factor for diffusion coefficient
\mathbf{r}	defined in Eq.(20) density
\mathbf{r}_{fact}	multiplication factor for density defined in Eq.(19)
(\mathbf{x}, \mathbf{h})	transformed coordinates in two dimensional case

Subscripts

c	pertaining to cold
eq	pertaining to equivalent value
f	pertaining to fluid
$fact$	pertaining to factor
h	pertaining to fluid
i	pertaining to interface
in	pertaining to inlet
ref	pertaining to reference value
s	pertaining to solid

References

1. A. Talja and E. Hansjosten, Results of Thermal Stratification Tests in a Horizontal Pipe Line at the HDR-Facility, Nucl. Eng. and Design, vol. 118, pp. 29-41, 1990.
2. L. Wolf, W. Hafner, M. Geiss, E. Hansjosten and G. Katzenmeier, Results of HDR-Experiments for Pipe Loads under Thermally Stratified Flow Conditions, Nucl. Eng. and Design, vol. 137, pp. 387-404, 1992.
3. W. R. Smith, D. S. Cassell and E. P. Schlereth. A Solution for the Temperature Distribution in a Pipe Wall Subjected to Internally Stratified Flow, Proceedings of the 1988 Joint ASME-ANS Nuclear Power Conf., Myrtle Beach, South Carolina, pp. 45-50, 1988.
4. H. K. Youm, M. H. Park and S. N. Kim, The Unsteady 2-D Numerical Analysis in a Horizontal Pipe with Thermal Stratification Phenomena, J. Korean Nucl. Soc., vol. 28, no. 1, pp. 27-35, 1996.
5. J. C. Jo, Y. I. Kim and S. K. Choi, Heat Transfer Analysis of Thermal Stratification in Piping Connected to Reactor Coolant System, In Proceedings of the 1st Korea-Japan Symposium on Nuclear Thermal Hydraulics and Safety, Paper no. WR-13, pp. 191-198, 1998.
6. Y. Abou-rjeily and G. Barois, Numerical Prediction of Stratified Pipe Flows in PWRs, Nucl. Eng. and Design, vol. 147, pp. 47-51, 1993.
7. F. Baron, M. Gabillard and C. Lacroix, Experimental Study and Three-Dimensional Prediction of Recirculating and Stratified Pipe Flow in PWR, Proc. of NURETH 4, Karlsruhe, pp. 1354-1361, 1989.
8. S. J. Baik, I. Y. Im and T. S. Ro, Thermal Stratification in the Surge Line of the Korean Next Generation Reactor, Proceedings of OECD NEA/WANO Special Meeting on Experience with Thermal Fatigue in LWR Piping Caused by Mixing and Stratification, Paris, France, 1998.
9. S. V. Patankar, Numerical Heat Transfer and Fluid Flow, McGraw-Hill, New York, 1980.
10. C. M. Rhie and W. L. Chow, Numerical Study of the Turbulent Flow Past an Airfoil with Trailing Edge Separation, AIAA J., vol. 21, no. 11, pp. 1525-1532, 1983.
11. J. P. Van Doormal and G. D. Raithby, Enhancements of the SIMPLE Method for Predicting Incompressible Fluid Flows, Numer. Heat Transfer, vol. 7, pp. 147-163, 1984.
12. S. Ushijima, Prediction of Thermal Stratification in a Curved Duct with 3D Body-Fitted Co-ordinates, Int. J. Numer. Methods Fluids, vol. 19, pp. 647-665, 1994.
13. S. K. Choi, H. Y. Nam, and J. C. Jo, Numerical Analysis of Evolution of Thermal Stratification in Curved Piping System, J. of KNS, Vol. 32, No.2, pp.169-179, 2000
14. J. C. Jo, Y. I. Kim, W. K. Shin, and S. K. Choi, Three-Dimensional Numerical Analysis of Thermally Stratified Flow in a Curved Piping System, ASME PVP-Vol. 414-1, pp 31-48, 2000

15. M. Peric, A Finite Volume Methods for the Prediction of Three Dimensional Fluid Flow in Complex Ducts, Ph.D. Thesis, Mechanical Engineering Department, Imperial College, London, 1985.
16. J. Zhu, A Low-Diffusive and Oscillation-Free Convection Scheme, Comm. Appl. Numer. Methods, vol. 7, pp.225-232, 1991.
17. J. H. Ferziger and M. Peric, Computational Methods for Fluid Dynamics, Springer Verlag, Berlin Heidelberg, Second Edition, pp. 134, 1999.
18. M. Majumdar, Role of Under-relaxation in Momentum Interpolation for Calculation of Flow with Non-staggered Grids, Numer. Heat Transfer, vol. 13, pp. 125-132, 1988.
19. S. K. Choi, Note on the Use of Momentum Interpolation Method for Unsteady Flows, Numer. Heat Transfer, Part A, vol. 36, pp. 545-550, 1999.

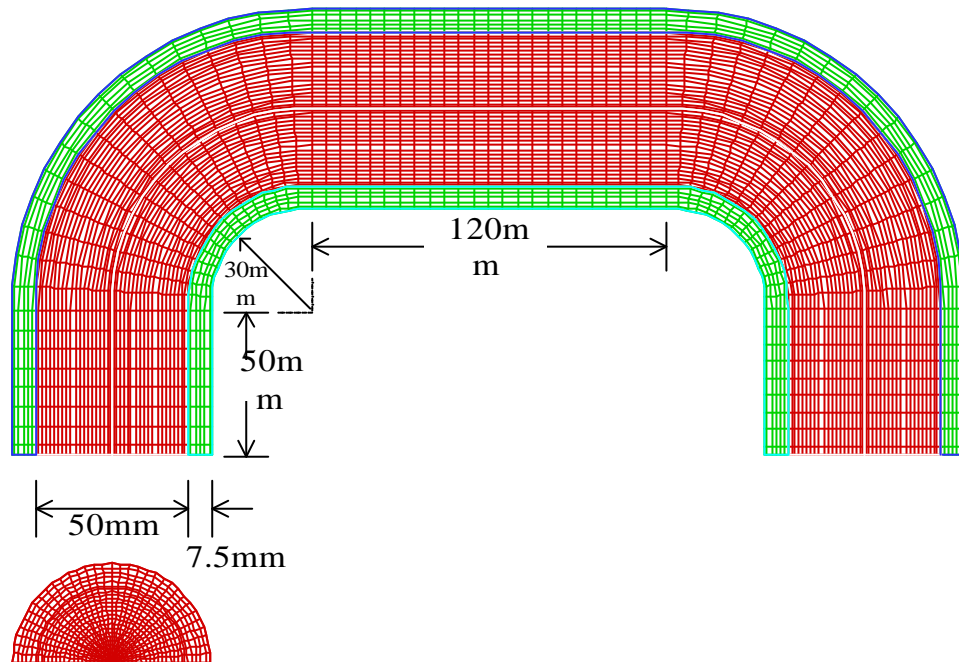


Fig. 1 Geometry and grids of the reversed U-pipe

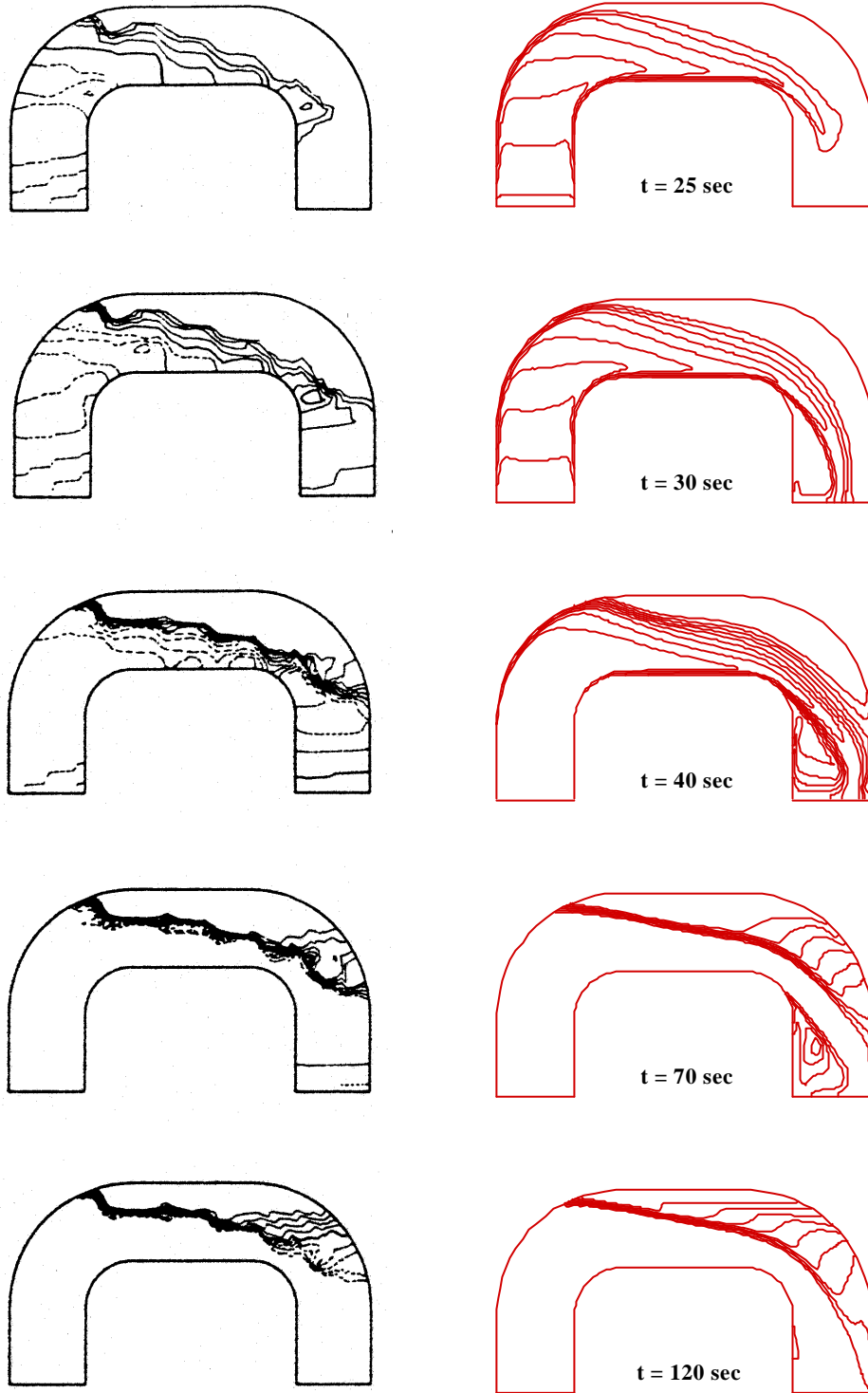
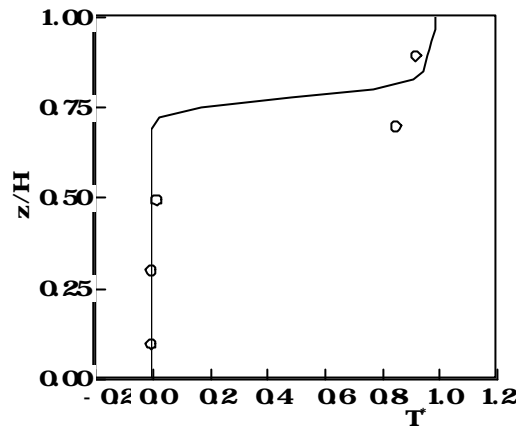
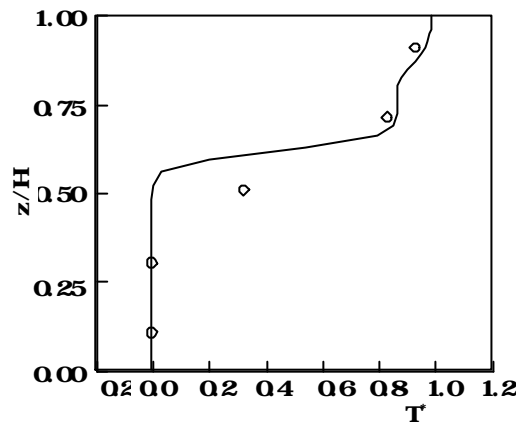


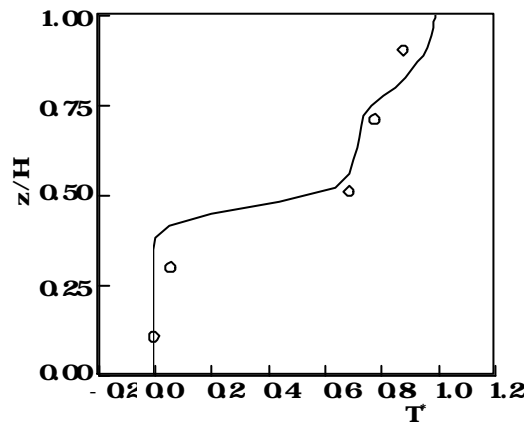
Fig. 2 Comparison between experiments and calculated results for temperature field (left: experimental results, right: calculated results)



(a) Section A



(b) Section B



(c) Section C

Fig. 3 Vertical temperature distributions at the three sections of the symmetry plane

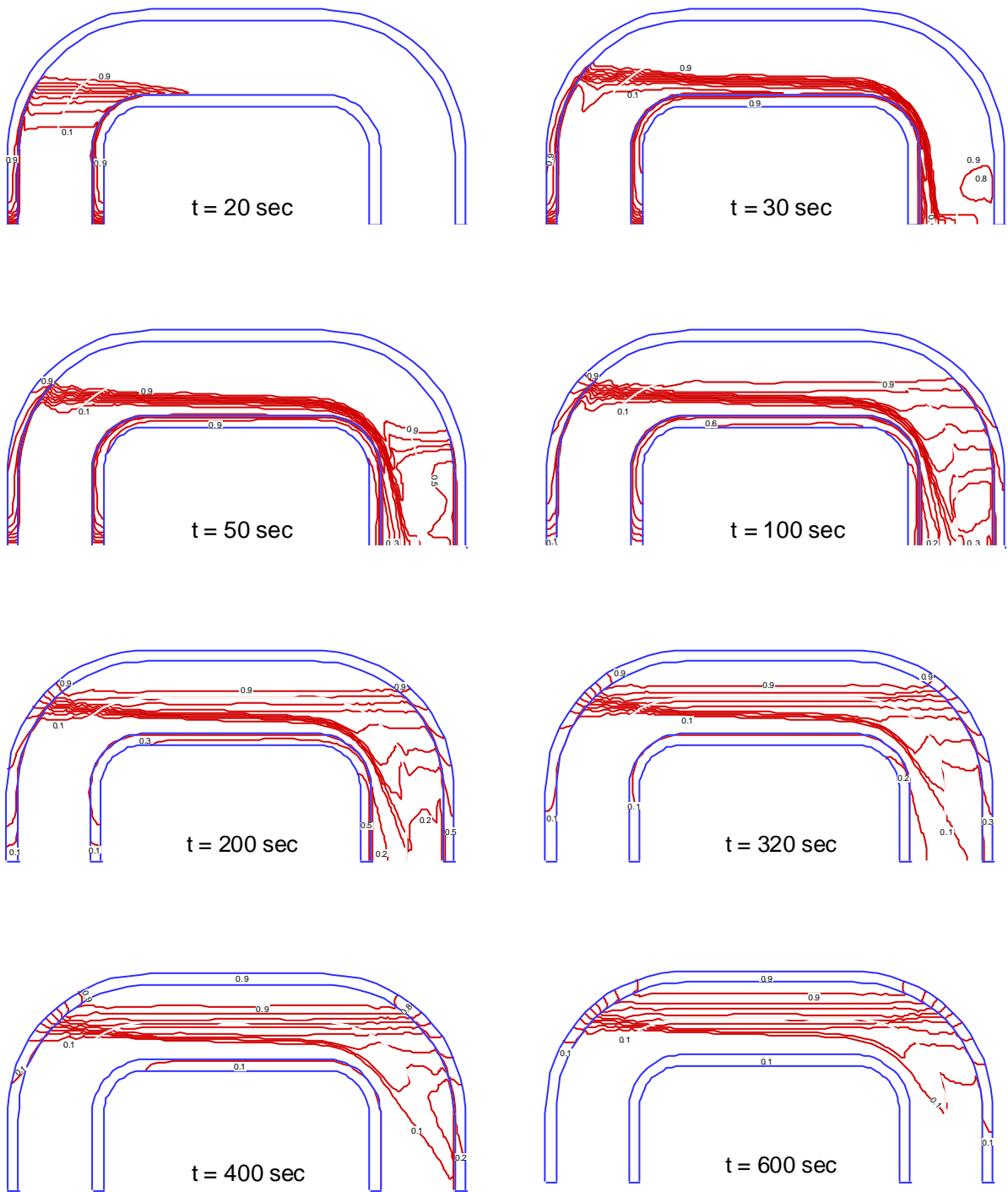


Fig. 4 Development of temperature field at the symmetry plane of the U-pipe

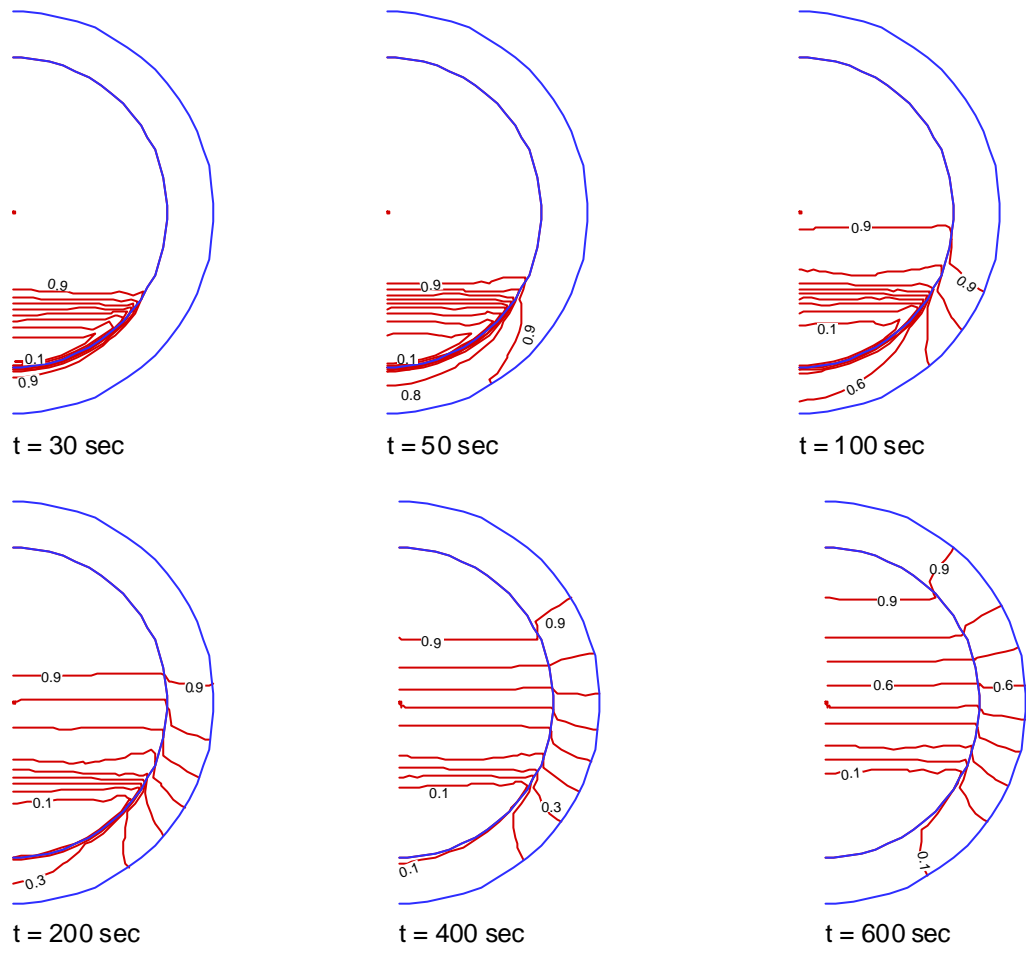


Fig. 5 Development of temperature field at the center cross-sectional plane of the U-pipe

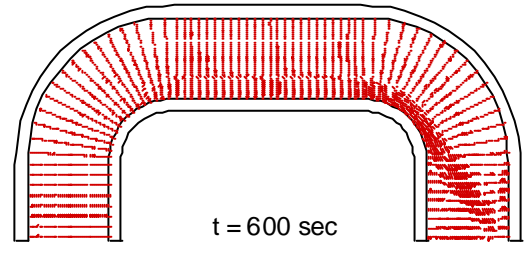
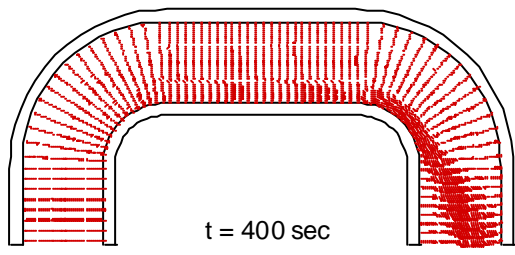
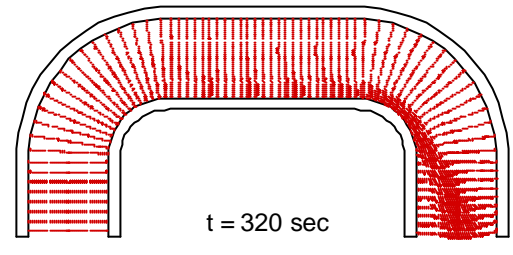
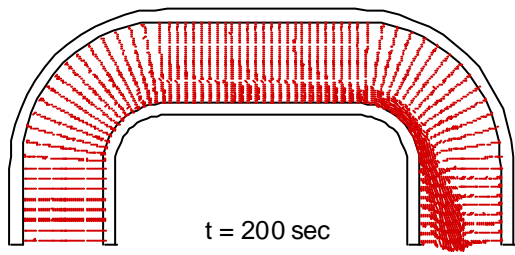
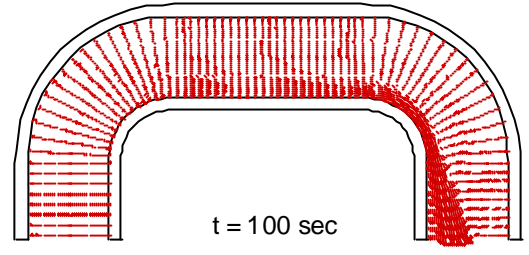
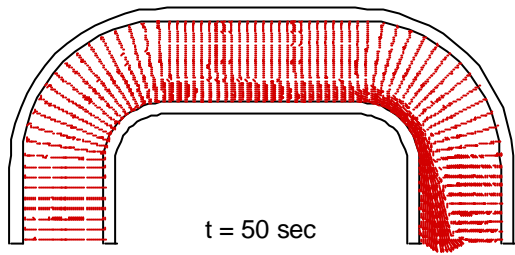
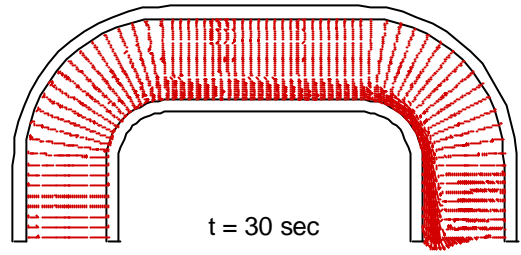
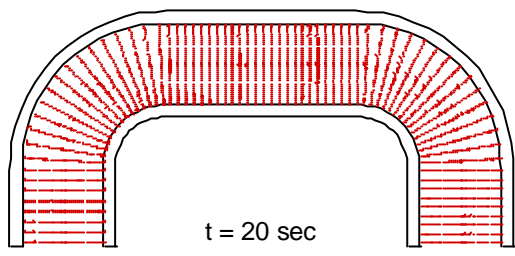


Fig. 6 Development of velocity field at the symmetry plane of the U-pipe

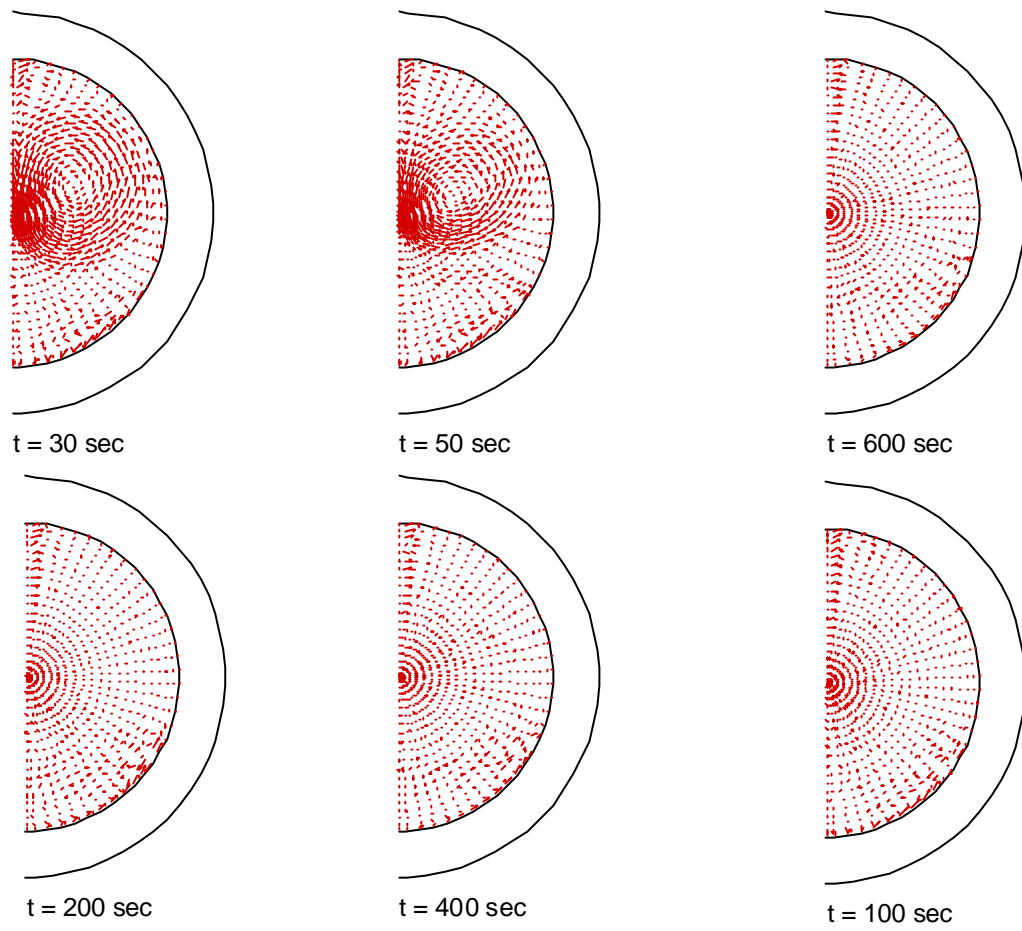


Fig. 7 Development of temperature field at the center cross-sectional plane of the U-pipe